Electronic Supplementary Material (ESI) for Chemical Communications

Supplementary Information for

Real-time observations on crystallization of gold nanorods into spiral or lamellar superlattices

Yong Xie,[a,b] Yongfei Jia,[a] Yujia Liang,[b] Shengming Guo,[b] Yinglu Ji,[c] Xiaochun Wu,*[,c] Ziyu Chen, *[,a] and Qian Liu,*[,b]

[a]Department of Physics/Key Laboratory of Micro-nano Measurement-Manipulation and Phsics (Minisry of Education), Beihang University, Beijing 100191, China

[b]Laboratory for Nanodevices, National Center for Nanoscience and Technology, Beijing 100190, China

[c]CAS Key Laboratory of Standardization and Measurement for Nanotechnology, National Center for Nanoscience and Technology, Beijing 100190, China

Method:

Materials. Hexadecyltrimethylammonium bromide (CTAB) was purchased from Amresco. All other chemicals used in the experiments were purchased from Sigma-Aldrich without further purification.

Preparation of GNPs. CTAB-coated gold nanoparticles (GNPs) were synthesized by a well-developed seed-mediated growth method. Gold nanospheres (diameter, 40.5 ± 6.7 nm), and gold nanorods (GNRs) with average aspect ratios of 3.4 ± 0.4 (length, 59.2 ± 6.3 nm; diameter, 17.3 ± 1.5 nm) and 4.1 ± 0.6 (length, 62.3 ± 7.7 nm; diameter, 15.5 ± 1.8 nm) were used as building blocks. After synthesis, GNPs were centrifuged (9000 rpm, 30 °C for 7 min) and re-dispersed in deionized water (18 MΩ·cm) to a concentration of about 0.5 nM with a CTAB concentration of about 1.0 mM, where the concentration of the GNPs was determined by Beer-Lambert law.

Preparation of Observed Samples. One milliliter of the GNPs solution was centrifuged for the second time (9000 rpm, 30 °C for 7 min) and the supernatant was removed as much as possible, the precipitate (about 10 μL) was re-dispersed with the as-prepared CTAB solution (5 mM, 5μL). Then the GNPs solutions were obtained with a CTAB concentration of 2.3 mM and particle concentration of about 33 nM.

Real-Time Observations of GNPs Self-Assemblies. Fifteen microliter of the GNPs solution was dropped onto a clean silicon wafer after a mild ultrasonic (about 1 min). The silicon wafers containing the GNPs were first put into a plastic petri dish, and then put again into a programmable temperature & humidity chamber for slow evaporation of the droplet with increasing humidity from 50 % to 85 % and temperature of 25 °C. The whole evaporation process took about 3.5 h. Next the droplet with a thin thickness of about 1 mm was moved carefully and rapidly to a glass slide fixed on a conventional

optical microscope (Leica DM2500). The observations were performed under the 100× objective lens with reflection mode, and the videos were acquired by screen recording software which simultaneously captured the images from the optical microscope.

SEM Imaging. Scanning electron microscope (SEM) images of the samples were acquired with a Hitachi S-4800 microscope operating at 10 kV for secondary electron imaging (SEI). The assembled geometry of the GNPs was determined both from the SEM images and the fast Fourier transform of the corresponding SEM image.

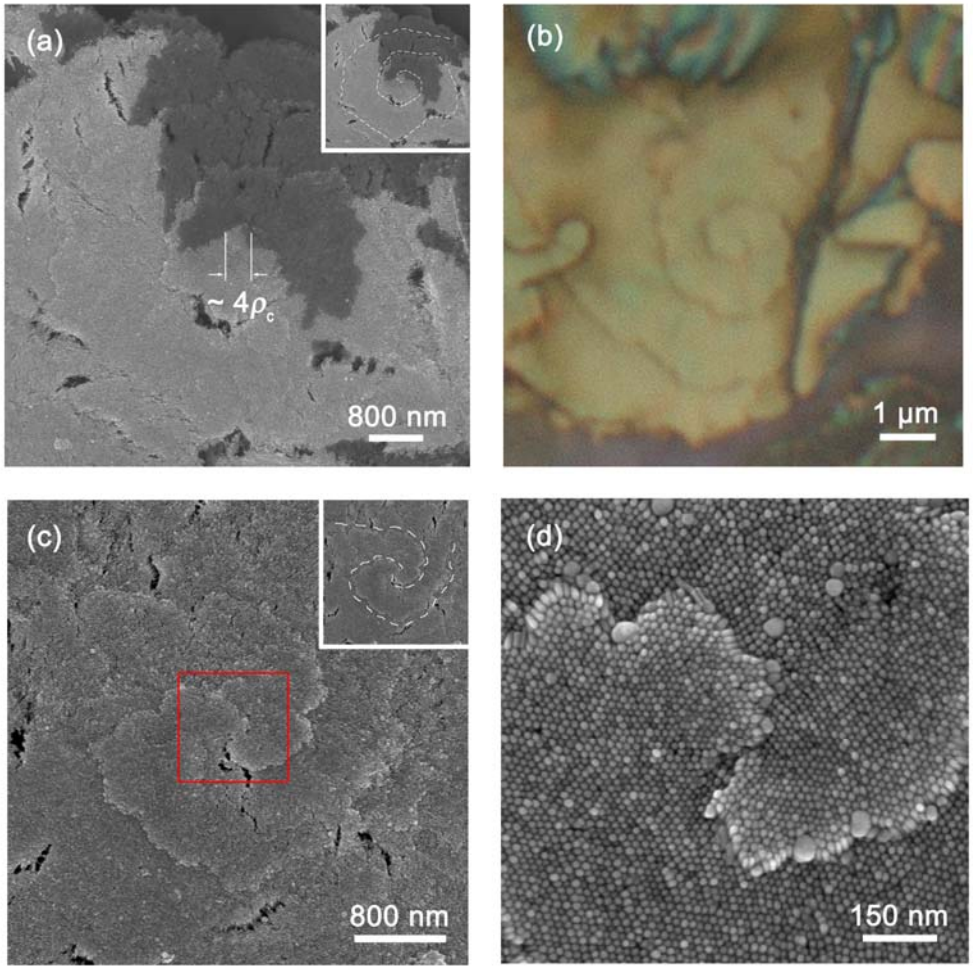

Figure S1. SEM and OM images of the diverse spiral superlattices observed in the

experiments. (a) The spiral superlattice with a transverse size of 6 μm and a vertical size of ~ 0.3 μm (4 layers of the standing GNRs). From the inset the boundary of the spiral superlattice is outlined by the dash line in order to guide the eye. According the crystal growth theory, we can in principle estimate the radius of the critical 2D nucleus ρ_c taking into account that the diameter of the first circle of the spiral superlattice is always equal to $4\rho_c$. The measured result here is about 100 nm (about 5 nanorods in close-packed, side-by-side alignment). (b) OM image of the superlattice, where the boundary of the spiral superlattice is seen clearly. (c) A special spiral superlattice formed by a pair of dislocations. The boundary of the superlattice is outlined by the dash line as shown in the inset. (d) Partial amplification of the special superlattice, where the two screw dislocations are presented clearly.

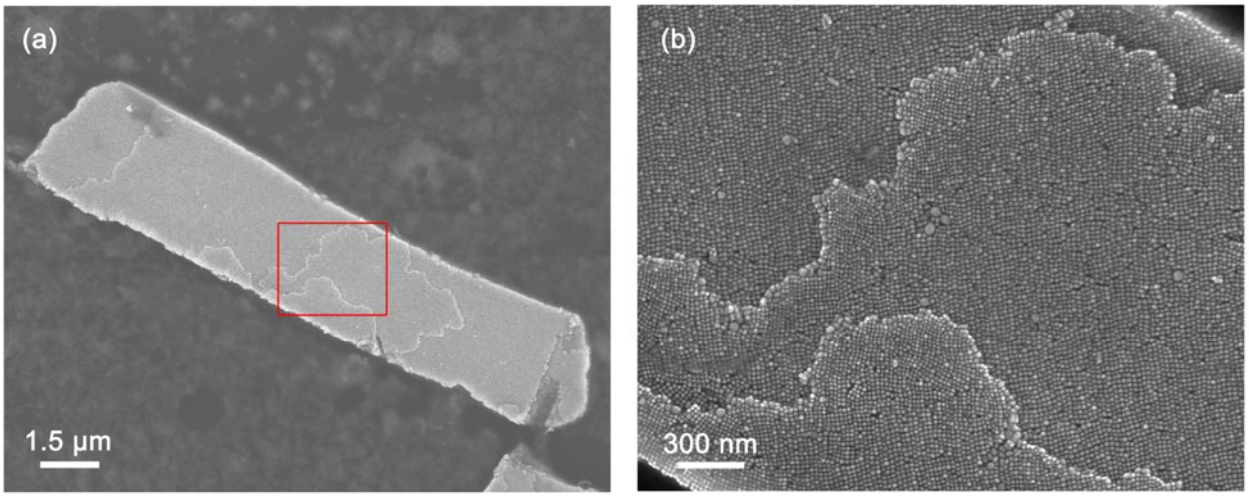

Figure S2. SEM images of another side of the laminar-2 superlattice. (a) A rectangular shape is shown on the whole with an obvious preferred growth orientation along the long sides. (b) Partial amplification of the superlattice, where a multilayer crystallization of close-packed, standing GNRs similar to that of the laminar-1 superlattices is observed.

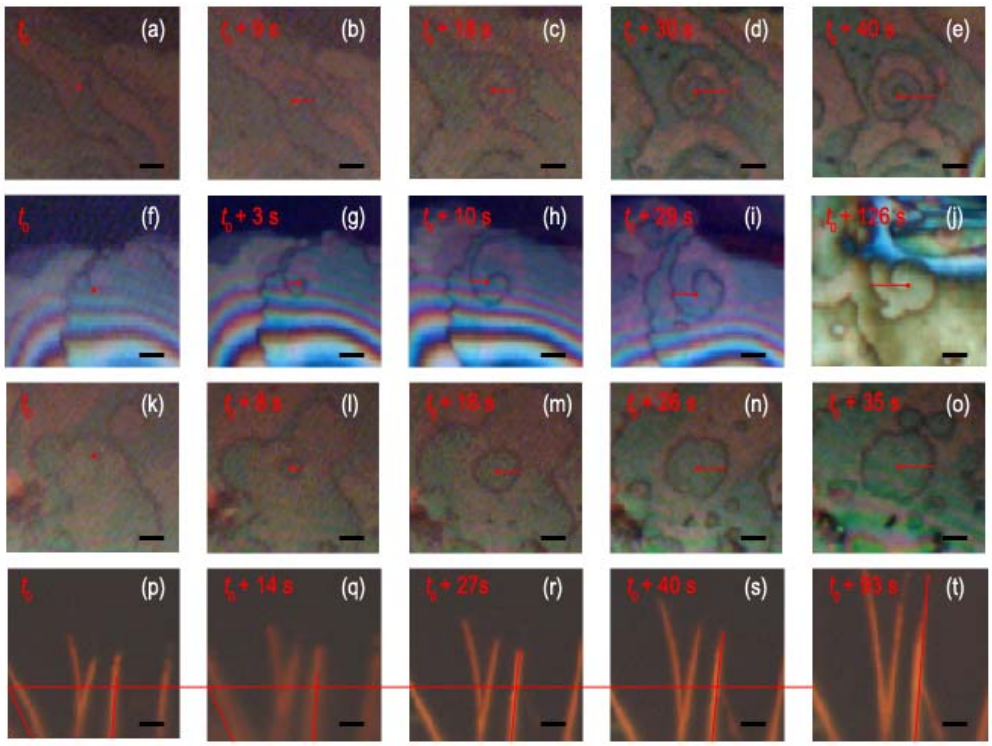

Figure S3. Lateral radius of curvature ρ and lateral length L of the superlattices. (a)-(o) The red lines are marked to show the lateral advance of radius of curvature of the spiral and the laminar-1 superlattices. Considering that the axial advance of the superlattices (about 0.06-0.3 μm) is far smaller than the lateral advance (0.2-3 μm) from the above results, therefore, we take the projection length to approximate the radius of curvature of the superlattices. (p)-(t) The red lines are marked to show the lateral advance of the laminar-2 superlattices. For reducing the error due to the panels clipping, the lengths of the lines are appropriately corrected.

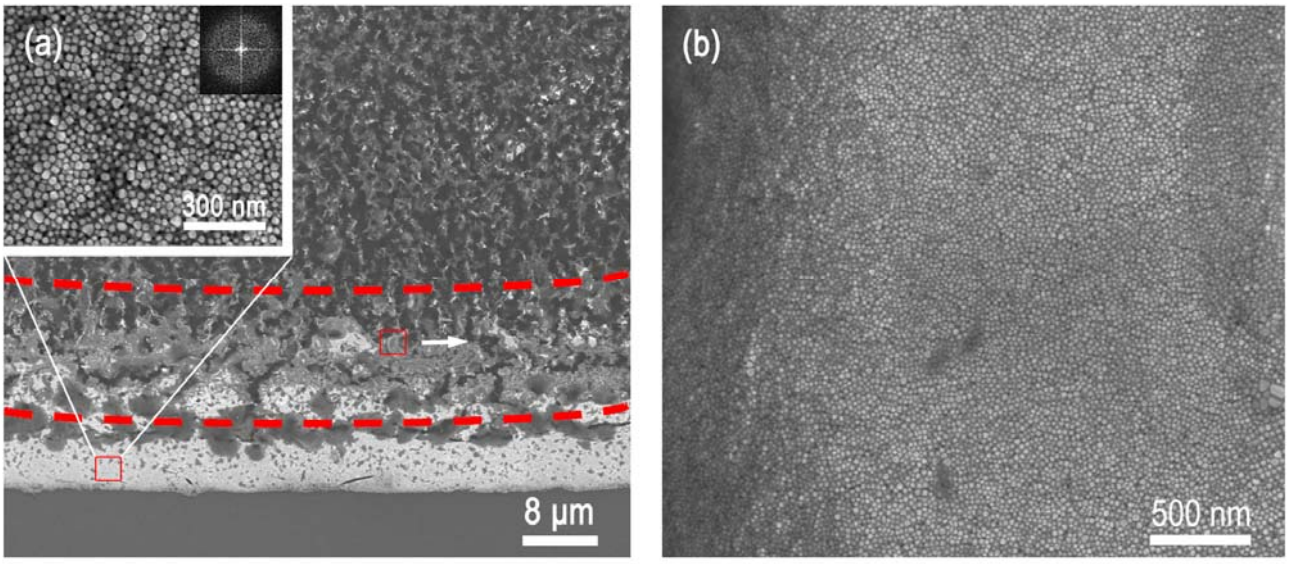

Figure S4. (a) Low-magnification SEM image of the "coffee stain" formed by gold nanospheres. The inset shows partial amplification of the nanospheres in the "coffee ring" and corresponding FFT of the inset image, suggesting an isotropic deposition. (b) SEM image of the close-packed gold nanospheres in the red dash-line marked region, indicating that no crystallization superstructures similar to the GNRs superlattices form.